JACS
JOURNAL OF THE AMERICAN CHEMICAL SOCIETY

Article

pubs.acs.org/JACS

Non-ribosomal Propeptide Precursor in Nocardicin A Biosynthesis Predicted from Adenylation Domain Specificity Dependent on the MbtH Family Protein NocI

Jeanne M. Davidsen, David M. Bartley,[†] and Craig A. Townsend*

Department of Chemistry, Johns Hopkins University, Baltimore, Maryland 21218, United States

Supporting Information

ABSTRACT: Nocardicin A is a monocyclic β-lactam isolated from the actinomycete *Nocardia uniformis* that shows moderate antibiotic activity against a broad spectrum of Gram-negative bacteria. The monobactams are of renewed interest due to emerging Gram-negative strains resistant to clinically available penicillins and cephalosporins. Like isopenicillin N, nocardicin A has a tripeptide core of non-ribosomal origin. Paradoxically, the nocardicin A gene cluster encodes two non-ribosomal peptide synthetases (NRPSs), NocA and NocB, predicted to encode five modules pointing to a pentapeptide precursor in nocardicin A biosynthesis, unless module skipping or other nonlinear reactions are occurring. Previous radiochemical incorporation experiments and bioinformatic analyses predict the incorporation of *p*-hydroxy-L-phenylglycine (L-*p*HPG) into positions 1, 3, and 5 and L-serine into position 4. No prediction could be made for position 2. Multidomain constructs of each module were heterologous expressed in *Escherichia coli* for determination of the adenylation domain (A-domain) substrate specificity using the ATP/PPi exchange assay. Three of the five A-domains, from modules 1, 2, and 4, required the addition of stoichiometric amounts of MbtH family protein NocI to detect exchange activity. On the basis of these analyses, the predicted product of the NocA and NocB NRPSs is L-*p*HPG−L-Arg−D-*p*HPG−L-Ser−L-*p*HPG, a pentapeptide. Despite being flanked by non-proteinogenic amino acids, proteolysis of this pentapeptide by trypsin yields two fragments from cleavage at the C terminus of the L-Arg residue. Thus, a proteolytic step is likely involved in the biosynthesis of nocardicin A, a rare but precedented editing event in the formation of non-ribosomal natural products that is supported by the identification of trypsin-encoding genes in *N. uniformis*.

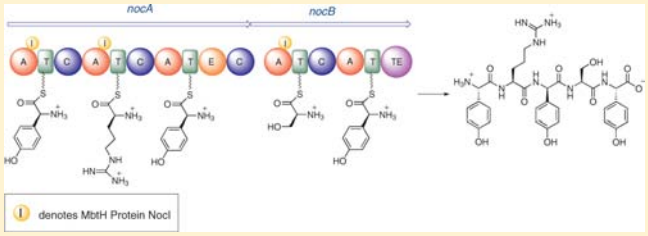

INTRODUCTION

The peptide core of many bioactive natural products, such as the antibiotics penicillin, vancomycin, and daptomycin, is biosynthesized by large modular proteins known as non-ribosomal peptide synthetases (NRPSs).[1] Interactions between NRPSs and other proteins are essential for overall catalytic function. NRPS proteins must interact with 4′-phosphopantetheinyl transferases (PPTases) that catalyze the transfer of a phosphopanethienyl side chain from coenzyme A (CoA) to the active site serine residue of each peptidyl carrier or thiolation (T) domain of the NRPS, converting apo-NRPS to its holo form.[1,2] In addition, there are increasing numbers of examples of associated biosynthetic proteins known to catalyze reactions, typically oxidations and halogenations, on T-domain-tethered substrates.[3,4] At the N- and C-termini of paired NRPS proteins, "COM domains", consisting of α-helical recognition units, are points of mutual interaction linking the product assembly reactions on each.[5] The importance of NRPS interaction with one or more auxiliary proteins for optimal activity is particularly well exemplified by recent discoveries that identify the crucial role of the MbtH family of proteins. The MbtH family comprise a group of relatively small proteins (~8−9 kDa) often found embedded in biosynthetic clusters for non-ribosomal peptide-derived secondary metabolites. They are collectively named for the protein identified in the mycobactin biosynthetic cluster of *Mycobacterium tuberculosis*.[6] In vivo studies of *Streptomyces coelicolor* A3(2) concluded that MbtH family proteins, CchK associated with the coelichelin gene cluster and CdaX associated with the calcium-dependent antibiotic (CDA) gene cluster, are indispensable for production of these secondary metabolites.[7] Another study demonstrated that heterologous expression of clorobiocin in *S. coelicolor* M512 was barely detectable upon the removal of all MbtH protein coding regions but complementation with *mbtH* genes *cchK*, *cdaX*, *cloY*, or *couY* (from the related coumermycin gene cluster) substantially restored production.[7,8]

Despite the prevalence of MbtH-encoding genes in NRPS-containing gene clusters and in vivo studies demonstrating their importance and structure determinations,[9,10] the role of these proteins in non-ribosomal peptide biosynthesis remained unclear until the ATP/PPi exchange activity of the NRPS protein VbsS was found to be dependent on its coexpression with VbsG, an MbtH protein encoded next to the NRPS in the vicibactin gene cluster.[11] A minimal NRPS module is three domains: an adenylation (A) domain, a thiolation (T) domain,

Received: August 7, 2012
Published: January 18, 2013

dx.doi.org/10.1021/ja307710d | J. Am. Chem. Soc. 2013, 135, 1749−1759

and a condensation (C) domain. A-domains activate their cognate substrate, typically an L-α-amino acid, by catalyzing the adenylation of the carboxylate moiety by reaction with ATP. This reaction is usually reversible and can be monitored by an ATP/PPi exchange assay. The activated substrate reacts with the terminal thiol group of the pantethienyl side chain of the T-domain, forming a thioester. C-domains catalyze peptide bond formation between the free amino group of the upstream T-domain-tethered aminoacylthioester with the downstream T-domain thioester. NRPSs usually terminate with a thioesterase (TE) domain, which catalyzes the release of the nascent peptide chain by hydrolysis or macrocyclization.

Several bioinformatic algorithms have been developed for substrate prediction of A-domains. The first algorithms were based on the crystal structure of PheA, the L-phenylalanine activating domain of the gramicidin NRPSs.[12] Structure studies of PheA show the substrate binding pocket and ATP binding region at the interface of the N-terminal and C-terminal domains of the enzyme. A-domain substrate prediction algorithms were derived by correlating the residues directly lining the substrate binding pocket to its cognate substrate.[13,14] More recent A-domain prediction algorithms have used transductive support vector machines (TSVMs) or hidden Markov Model (HMM) methodologies to improve prediction capabilities.[15−17]

The activation of ATP/PPi exchange activity in VbsS by VbsG suggests the MbtH protein interacts with the A-domain of VbsS. The contribution of MbtH homologues VioN, CmnN, and PacJ to the activity of NRPSs involved in the biosynthesis of viomycin, capreomycin, and pacidamycin, respectively, were subsequently reported.[18,19] CmnN and VioN were found to be necessary to activate the ATP/PPi exchange reactions in the β-lysine activating modules of CmnO and VioO and modules 1 and 2 from CmnA but are not required for ATP/PPi exchange in the A-domains of NRPSs CmnF and CmnG. PacJ is required for activation of ATP/PPi exchange in PacL. The mechanism for A-domain activation by MbtH proteins remains unclear. Kinetic measurements of the NovH tyrosine activating domain in novobiocin biosynthesis indicated that the K_m and the turnover number measured for NovH were dissimilar when paired with different but complementary MbtH proteins CloY and YbdZ.[20]

Nocardicin A is the most potent of the nocardicin antibiotic isolated from *N. uniformis* subsp. *tsuyamanensis* ATCC 21806, with activity against Gram-negative bacteria. Nocardicin A has also been isolated from other actinomycetes, including *Actinosynnema mirum*.[21] The genus *Actinosynnema* is characterized by the formation of synnemata from the substrate mycelium, at the tip of which, zoospores are produced.[22] Classical morphological comparison of *N. uniformis* ATCC 21806 to *A. mirum* strain NR 0364 revealed a high degree of similarity in the formation of synnemata and zoospores suggesting that it should be reclassified into the *Actinosynnema* genus.[21]

While both *A. mirum* and *N. uniformis* produce nocardicin A and have nearly identical gene clusters, the biosynthetic pathway has only been studied in *N. uniformis*. The structures of all the nocardicins isolated from *N. uniformis* contain a tripeptide core known to be derived from two units of *p*-hydroxy-L-phenylglycine (L-*p*HPG) and one unit of L-Ser.[23] While a three module NPRS would be expected in the nocardicin A gene cluster, two NRPSs, NocA and NocB, together containing five modules were found.[24] Recent in vivo mutagenesis experiments indicate that each of these five modules is essential, demonstrating that module skipping is not likely occurring and implying the formation of a pentapeptide precursor in nocardicin A biosynthesis by the conventional linear paradigm.[24] Determination of each A-domain substrate specificity would provide the identity of this putative pentapeptide and may suggest mechanisms by which subsequent truncation occurs to form the tripeptide backbone of the nocardicins. Bioinformatic algorithms have predicted L-*p*HPG to be the preferred substrate for A1, A3, and A5 and L-Ser to be the preferred substrate for A4.[13] The substrate specificity for A2 has been more problematic with low confidence predictions ranging from L-ornithine to L-δ-*N*-hydroxyornithine,[24] "a large amino acid such as L-Orn, L-Lys, or L-Arg", a hydrophilic amino acid, L-Asp, L-Asn, L-Glu, or L-Gln, or L-Arg.[15,25] The inability to obtain clear experimental data for A2 has prevented identification of the presumed pentapeptide and left unknown whether the tripeptide backbone of nocardicin A originates from modules 1−3 or 3−5.

Among the proteins encoded by the nocardicin A biosynthetic cluster, NocI, a small 74 amino acid protein, shows clear homology to the MbtH family of proteins, and 2.3 kbp upstream of the cluster, a 73 amino acid paralogue encoded by *nocP* is found. In this study, we report MbtH protein NocI is required for ATP/PPi exchange to be observed in three of the five A-domains of NocA and NocB. Surprisingly, the MbtH protein encoded just upstream of the cluster, NocP, was found to only partially complement NocI. The A-domain•NocI/NocP protein interaction was further characterized by coexpression studies. High-performance liquid chromatography (HPLC) and binding analyses of dependent modules coexpressed with NocI indicate a 1:1 stoichiometry. Determining the function of NocI was requisite to experimentally demonstrating the identities of the amino acids recognized and activated by each module of NocA and NocB. As a result, a pentapeptide precursor can now be proposed for nocardicin A biosynthesis, as well as possible mechanisms for proteolysis to a tripeptide later in the biosynthetic pathway.

RESULTS

A-Domain Specificities of NocA and NocB. Heterologous expression of a multidomain construct from each module of NocA and NocB in *Escherichia coli* was pursued so that the substrate specificity could be experimentally determined for each A-domain using the standard ATP/PPi exchange assay. For all modules, except module 2, each construct was cloned into pET28b(+) for expression of C-terminal His_6 fusion proteins in *E. coli* BL21(DE3) Rosetta 2 cells and purification by NTA affinity chromatography and Q-Sepharose ion-exchange chromatography. Yields typically ranged 0.5−1 mg protein/L culture. Because this expression protocol failed for several constructs of module 2, the A_2T_2−His_6 coding sequence was cloned into pMALc2x for expression of an N-terminal maltose binding protein (MBP) fusion protein. Heterologous expression of MBP−A_2T_2−His_6 in *E.coli* BL21(DE3) Rosetta 2 and isolation by NTA affinity chromatography yielded 2−3 mg protein/L culture. Protein products were confirmed by matrix-assisted laser desorption ionization mass spectrometry (MALDI MS) analysis of trypsin digests.

Bioinformatic analysis of the A-domains of modules 1, 3, and 5 predicted L-*p*HPG to be their preferred substrate although protein sequence alignment of these three A-domains highlights a long linker region between motifs 2 and 3 in the A1 domain

that is not found in the A3 or A5 domains.[24] The ATP/PPi exchange assay results for A_1T_1–His_6, $A_3T_3E_3C_4$–His_6, and $C_5A_5T_5TE$–His_6 are shown in Figure 1A. Very strong ATP/PPi

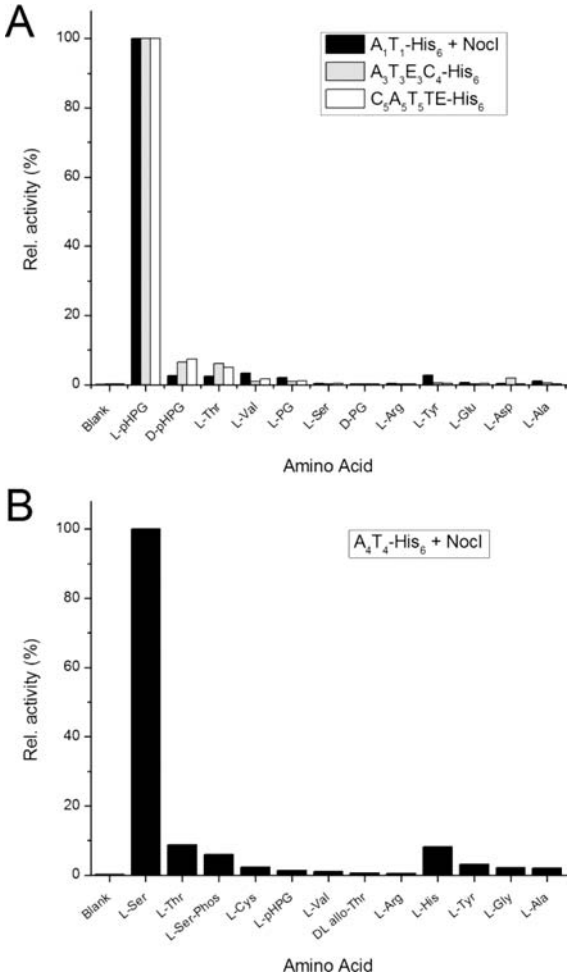

Figure 1. Representative results of the ATP/PPi exchange assay for L-*p*HPG activating modules A_1T_1–His_6, $A_3T_3E_3C_4$–His_6, and $C_5A_5T_5TE$–His_6 and L-serine activating module A_4T_4–His_6 at 0.5 μM. For modules A_1T_1–His_6 and A_4T_4–His_6 that require addition of a MbtH protein for activity, His_6–NocI was added at 2 μM final concentration. All assays were performed at room temperature.

exchange was observed in the presence of L-*p*HPG for these three modules with a marked lack of activity for any other amino acid substrate. Although some exchange above background was observed with D-*p*HPG as substrate (ca. 6% relative to L-*p*HPG), this observed activity is likely the result of a small L-isomer impurity. It should be noted that no exchange activity was observed for closely related analogues of *p*HPG such as L-phenylglycine (PG), D-PG, D/L-4-fluorophenylglycine (FPG), or D/L-4-chlorophenylglycine (ClPG), a further indication of the high specificity of these A-domains.

For the present discussion, however, it is important to note that, despite the similarity of the amino acid binding pockets of A1, A3, and A5, ATP/PPi exchange in A_1T_1–His_6 was only observed in the presence of the MbtH proteins NocI or NocP. Of the three L-*p*HPG activating modules, ATP/PPi exchange was dependent on stoichiometric amounts of MbtH protein only in A_1T_1–His_6. The addition of NocI to $A_3T_3E_3C_4$–His_6 and $C_5A_5T_5TE$–His_6 had no effect on the ATP/PPi exchange reaction under identical experimental conditions.

The substrate binding pocket of the A4 domain in NocB was predicted to activate L-serine by several algorithms and was consistent with past experiments that established the β-lactam ring of nocardicin A is derived from L-serine.[23] Initial ATP/PPi exchange assays of A_4T_4–His_6 failed to demonstrate any significant activity in the presence of any amino acid. As observed in experiments with A_1T_1–His_6, A_4T_4–His_6 was also dependent on the presence of stoichiometric amounts of NocI for the observation of ATP/PPi exchange with its preferred substrate, L-serine, as shown in Figure 1B.

Substrate determination for the A2 domain has been the most difficult to achieve of the five modules, as noted earlier. Recently, the A6 domain of the lysobactin NRPS was characterized to activate L-Arg, independent of the presence of a MbtH protein.[26] A2 shares the eight residue L-Arg binding pocket signature with this lysobactin A-domain, as well as showing good overall similarity to it (40.2% identical, 55.8% similar). Upon expression and purification of MBP–A_2T_2–His_6, initial ATP/PPi exchange experiments conducted under conditions used to characterize A_1T_1–His_6, $A_3T_3E_3C_4$–His_6, A_4T_4–His_6, and $C_5A_5T_5TE$–His_6 demonstrated only weak exchange activity and poor selectivity in the presence of small hydrophobic amino acids such as L-Val, L-Leu, and L-Ile and no exchange activity for L-Arg. As depicted in Figure 2A, the observation of L-Arg dependent ATP/PPi exchange was only observed under altered assay conditions[26] involving a 10-fold higher concentration of protein, conducting experiments at 30 °C instead of room temperature (~23 °C), and the addition of a 2-fold excess of NocI to the assay. Of note, under these conditions, significant ATP/PPi exchange was also observed for the hydrophobic amino acids L-Val, L-Leu, L-Ile, and L-Phe, but this activity was not dependent on the addition of the MbtH protein NocI. The dramatic activation of ATP/PPi exchange by NocI in the presence of L-Arg compared to the small hydrophobic amino acids is seen in a difference plot (Figure 2B). Also, unlike the lysobactin A6 domain, ATP/PPi exchange activity by MBP–A_2T_2–His_6 was not observed for D-Arg, and ATP/PPi exchange activity was not observed for similar amino acids predicted from bioinformatics such as L-ornithine, L-*δ*-*N*-hydroxyornithine, L-*δ*-*N*-acetyl-*δ*-*N*-hydroxyornithine, or L-Lys.

Interaction of MbtH Proteins NocI and NocP with Nocardicin A-Domains. To understand further its interaction with each nocardicin module, NocI was cloned into pCDFDuet for heterologous expression as an N-terminal His_6 fusion protein as well as an untagged protein in *E. coli*. In addition, untagged NocI for in vitro experiments was prepared by heterologous expression of NocI fused to an intein attached to a chitin binding domain (CBD) tag followed by binding to chitin-binding affinity resin and cleavage of the CBD tag from NocI with DTT. The rate of ATP/PPi exchange as a function of NocI (untagged) concentration for 0.5 μM concentrations of A_1T_1–His_6 and A_4T_4–His_6 is shown in Figure 3. Although the overall exchange rate is much higher for A_1T_1–His_6 compared to A_4T_4–His_6, both hyperbolic curves plateau at ~2 μM NocI and have K_m values of 0.41 μM and 0.59 μM, respectively. In a similar experiment with $A_3T_3E_3C_4$–His_6 and $C_5A_5T_5TE$–His_6, NocI had no effect on the rate of ATP/PPi exchange of their preferred substrate L-*p*HPG. This observation was supported by analysis of the ATP/PPi exchange reaction for proteins isolated from an $A_3T_3E_3C_4$–His_6/A_4T_4–His_6 coexpression experiment. Addition of His_6–NocI to the assay greatly enhanced ATP/PPi

dx.doi.org/10.1021/ja307710d | J. Am. Chem. Soc. 2013, 135, 1749–1759

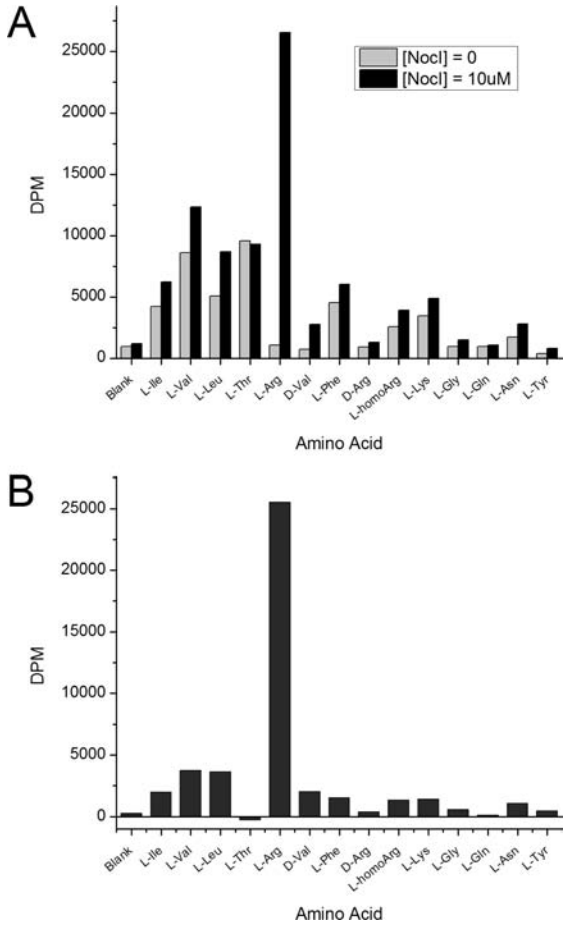

Figure 2. Representative results of the ATP/PPi exchange assay for 5 μM L-Arg activating MBP−A_2T_2−His_6 performed at 30 °C. (A) Data plot for activity with and without addition of 10 μM His_6−NocI. (B) Difference plot: the activity of MBP−A_2T_2−His_6 with His_6−NocI with the background activity seen in the absence of His_6−NocI subtracted.

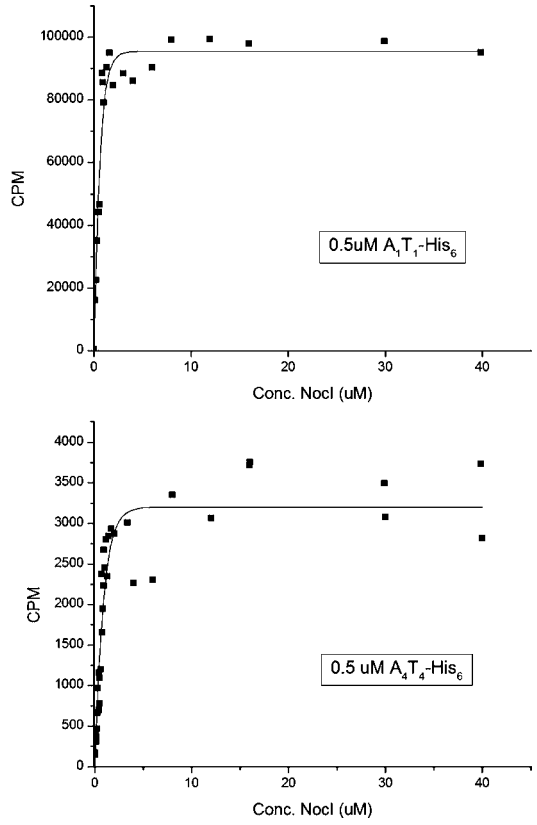

Figure 3. ATP/PPi exchange rate for modules A_1T_1−His_6 (A) and A_4T_4−His_6 (B) as a function of increasing NocI (untagged) concentration. The fitted line was generated by curve fitting to the Box Lucas model equation: $y = a(1 - b^x)$ using OriginLab software version 8.6.

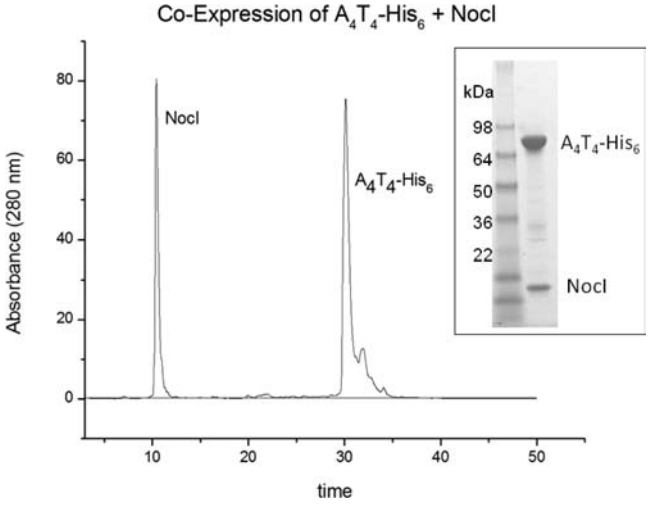

Figure 4. HPLC chromatogram and SDS-PAGE gel (inset) of A_4T_4−His_6/NocI (untagged) coexpression, purified by NTA affinity chromatography.

exchange activity observed in the presence of L-Ser but showed little effect on the activity observed in the presence of L-*p*HPG.

To characterize further the interaction between each module and NocI, untagged NocI was coexpressed with each C-terminally labeled His_6 module protein. Following expression, the individual modules were isolated using the standard NTA affinity isolation protocol. Sodium dodecyl sulfate polyacrylamide gel electrophoresis (SDS-PAGE) analysis suggested that untagged NocI coeluted (or was pulled down) by A_1T_1−His_6, MBP−A_2T_2−His_6, and A_4T_4−His_6, indicating strong interaction. This interaction was not observed during the purifications of $A_3T_3E_3C_4$−His_6 or $C_5A_5T_5TE$−His_6 coexpressed with NocI. For a more quantitative evaluation, the final eluant for each coexpression reaction was denatured by the addition of urea and analyzed by HPLC to confirm the presence of NocI and estimate the module/NocI stoichiometry. The chromatogram and SDS-PAGE gel for the A_4T_4−His_6/NocI coexpression are shown in Figure 4. As expected owing to its smaller size, NocI elutes first followed much later by A_4T_4−His_6. On the basis of the area of each peak and the molar absorptivity of each protein calculated by Vector NTI, the A_4T_4−His_6/NocI and A_1T_1−His_6/NocI stoichiometric ratios were each calculated to be 1:1. The observation of a 1:1 stoichiometic relationship is consistent with the shape of the activity curves shown in Figure 3. Due to the complexity of the HPLC chromatogram, the stoichiometry of the MBP−A_2T_2−His_6/NocI coexpression could not be confidently determined. Chromatograms for the coexpression of $A_3T_3E_3C_4$−His_6/NocI and $C_5A_5T_5TE$−His_6/NocI failed to show any peak in the NocI region, consistent with SDS-PAGE analysis and in keeping with the absence of a strong binding between A3 or A5 with NocI.

dx.doi.org/10.1021/ja307710d | J. Am. Chem. Soc. 2013, 135, 1749−1759

The ability to reconstitute the activity of the A_1T_1–His_6•NocI and A_4T_4–His_6•NocI coexpressed proteins by combinations of individually expressed NocI, A_1T_1–His_6, and A_4T_4–His_6 was also investigated, based on the HPLC response factors for each protein. The activity of reconstituted A_4T_4–His_6 and NocI was ∼50% of the coexpressed A_4T_4–His_6•NocI sample. For A_1T_1–His_6, the activity of the reconstituted proteins was ∼70% of the coexpressed A_1T_1–His_6•NocI sample.

To investigate the ability of an MbtH family protein generated outside the nocardicin cluster to complement NocI, NocP was heterologously expressed in *E.coli* as an N-terminal His_6 fusion protein from pET28b(+) and as an untagged form from pCDFDuet. Several experiments were carried out to compare the activity of His_6–NocI to His_6–NocP with A_1T_1–His_6, MBP–A_2T_2–His_6 and A_4T_4–His_6. Interestingly, His_6–NocP activated ATP/PPi exchange activity in A_1T_1–His_6 and A_4T_4–His_6 but not in MBP–A_2T_2–His_6. Furthermore, analysis of the coexpression product of NocP (untagged) with MBP–A_2T_2–His_6 by HPLC indicated that NocP does not form a strong interaction with MBP–A_2T_2–His_6 yet NocI was pulled down by MBP–A_2T_2–His_6. Together, these results indicate that NocP cannot fully complement NocI.

Phylogenic Analysis of *N. uniformis* ATCC 21806. To evaluate the phylogenic similarity of *N. uniformis* to *A. mirum*, 16S rDNA was amplified from *N. uniformis* for sequencing and was submitted to GenBank for comparison. The 16S rDNA (1508 nt) isolated from *N. uniformis* was found to be identical to *A. mirum* 16S rDNA (GenBank accession number CP001630.1) except for one polymorphism, and they are thus identical based on standard classification criteria.[27,28]

Genome Mining for Trypsin Proteases in *A. mirum*. The predicted pentapeptide formed by NocA and NocB, L-*p*HPG–L-Arg–D-*p*HPG–L-Ser–L-*p*HPG, requires trimming at the C-terminus of L-Arg during nocardicin A biosynthesis. Trypsins specifically cleave peptides at the C-terminus of L-Lys and L-Arg and have been isolated from bacteria as well as mammals.[29] BLASTP[30] analysis of the *A. mirum* complete genome revealed at least five probable trypsins, three of which have ≥38% identity ≥50% similarity to well-characterized trypsins from *Streptomyces griseus* and *Saccharopolyspora erythraeus*.[31,32]

To confirm the presence of the typsin encoding genes mined from the *A. mirum* genome in our strain, three trypsin proteases, ACU39320, ACU39665, and ACU39678, were selected for polymerase chain reaction (PCR) amplification and sequence comparison. All three were successfully amplified from *N. unformis* gDNA and confirmed by sequencing analysis to be identical to the corresponding *A. mirum* genes.

Trypsin Proteolysis of Pentapeptide Precursor. The predicted product of the nocardicin NRPSs, L-*p*HPG–L-Arg–D-*p*HPG–L-Ser–L-*p*HPG, was purchased for evaluation. HPLC analysis of a pentapeptide trypsin reaction mixture showed the disappearance of the pentapeptide peak and the corresponding appearance of two new peaks with retention times significantly shorter than the starting material. (Supporting Information, Figure S1) Liquid chromatography–mass spectrometry/time-of-flight (LC-MS/TOF) analysis of the earliest eluting peak indicated a mass of 324.17 Da, which corresponds to the (M + H) of the L-*p*HPG–L-Arg dipeptide. The second peak has a mass of 404.15 Da consistent with the (M + H) of the predicted D-*p*HPG–L-Ser–L-*p*HPG tripeptide. Thus, this analysis indicates complete cleavage at the C-terminus of the L-Arg residue, as expected for trypsinolysis, despite its being flanked by two nonproteinogenic amino acids, one in the D-configuration.

■ DISCUSSION

NRPS A-domains constitute a subfamily of the ANL superfamily of adenylating enzymes, which also includes acyl and aryl CoA synthetases and firefly luciferase. ANL enzymes catalyze two reactions, the adenylation of a substrate carboxylate to form a high energy acyl-AMP intermediate followed by an acyl substitution reaction with the pantetheinyl side chain of a T-domain in the NRPS A-domain subfamily, reaction with CoA by members of the acyl and aryl CoA synthetases subfamily, or oxidative decarboxylation followed by the generation of light in the firefly luciferase subfamily.[33] Structure studies of the PheA domain, the initial A-domain in gramicidin S synthetase, show a two-domain structure with a larger N-terminal domain (∼430 residues) and a smaller C-terminal domain (∼100 residues) with a connecting loop (A8 loop) between the two domains, which is a theme repeated throughout the ANL superfamily.[12] The PheA domain, crystallized with phenylalanine and AMP in the active site, is in the adenylation conformation, in which the conserved and essential A10 lysine forms hydrogen bonds with the oxygen atom in the ribose ring and the 5′ bridging oxygen of AMP and the carboxylate oxygen of phenylalanine.[12] The alternation of conformational states during the catalytic cycle of the A-domain was first supported by crystal structure studies of DltA, a D-alanyl carrier protein ligase from *Bacillus cereus* that catalyzes the adenylation and thioesterification reaction of D-alanine in cell wall biosynthesis, which has been captured in several conformations.[34−36] This model is supported by recent crystal structure studies of PA1221, a two-domain (A–T) NRPS in both the adenylation and thioester-forming conformations.[37] Experimental evidence suggests that ANLs undergo a major ∼140° conformational change between the adenylation and thioester reaction conformations, an observation that is supported by the recent solution of 4-chlorobenzoate•CoA ligase crystal structure captured in both the adenylate-forming and the thioester-forming conformations.[38] Lacking a crystal structure of firefly luciferase trapped in the second, light producing configuration, Brachini et al. performed an experiment in which the N- and C-terminal domains were trapped in this arrangement by chemical cross-linking of two cysteine residues, one from each domain, with 1,2-bis(maleimidoethane). In the trapped configurational state, bioluminescence was not observed unless synthetic dehydroluciferyl–AMP substrate was added to bypass the inactivated adenylation half-step.[39] Analysis of the recently solved structure of this cross-linked firefly luciferase finds it locked into a conformation similar to the thioester formation step in acyl CoA synthetases.[40]

Based on these studies, it has been proposed that A-domains may adopt at least three conformations: an open conformation in the absence of substrates, the adenylation conformation upon the binding of an amino acid substrate and ATP, and the thioester conformation, a 140° rotation from the adenylation conformation, that occurs upon the release of PPi.[34] Both nocardicin synthetase initiation domains A1 and A4 and elongation domain A2 failed to catalyze an ATP/PPi exchange reaction in the presence of their preferred amino acid substrates until the addition of NocI.

On the basis of the studies described above, it is postulated that these domains can be "trapped" in a state in which one or

dx.doi.org/10.1021/ja307710d | J. Am. Chem. Soc. 2013, 135, 1749−1759

more of the substrate-binding, adenylation, or thioester-forming conformations is blocked in a way that is relieved by NocI or other compatible MbtH protein.

Expanding on this hypothesis, pull-down studies reported here support a 1:1 stoichiometric relationship between NocI and an interacting A-domain. In secondary metabolism, there is a set of glycosyltransferases (GTs) whose activity requires a stoichiometric amount of a partner protein for activity. DesVII, a GT involved in macrolide biosynthesis from *S. venezuelae,* requires DesVIII for activity, and these two proteins were shown to form a tight 1:1 complex when copurified.[41] Analogously, EryCIII, a GT required for erythromycin D biosynthesis, requires partner protein EryCII for activity, and a the structure of the complex formed by these two proteins, a dimer of heterodimers, has been recently solved.[42] Analytical gel chromatographic analysis of the tyrosine adenylating enzyme SimH coupled to its cognate MbtH protein, SimY, also indicates the formation of a heterotetrameric complex.[20] The EryCIII•EryCII interface is characterized where the N-terminal helix of EryCII is sitting in a groove formed by three helices in EryCIII and stabilized by electrostatic interactions. This observation suggests two roles for the partner protein EryCII: stabilization of the GT and allosteric regulation.[42] It appears that MbtH proteins also might share these two roles to varying degrees. While neither NocI nor NocP was required for the expression of modules from NocA or NocB in *E. coli*, the requirement for coexpression of a cognate MbtH protein with an NRPS protein domain in *E. coli* has been reported in several cases suggesting a stabilization role for the MbtH protein in these instances.[11,43−45]

The ability to reconstitute the A-domain•MbtH protein interaction in vitro with separately expressed proteins has been evaluated. Measurements of A_4T_4−His_6 and A_1T_1−His_6 reconstituted with NocI indicated ATP/PPi exchange activity of 50−70% of the activity observed for an equivalent amount of the coexpressed proteins. These differences in activity may be due to the presence of impurities or unfolded proteins, skewing the protein quantitation. Similar reconstitution experiments on different systems have shown varying results. The coexpression of CloH and CloY resulted in a protein mixture that was ∼50% less active than the reconstitution of separately expressed proteins.[20] Conversely, the coexpressed proteins CmnO and CmnN resulted in a dramatically more active mixture than when the equivalent amounts of CmnO and CmnN from single expressions were combined.[18]

Of the three L-*p*HPG activating domains in NocA and NocB, only A1 is dependent on an MbtH protein for activation. Alignments of the nocardicin NRPS domains were performed to determine a conserved region that might be responsible for interaction with MbtH proteins (Supporting Information, Figure S2). On the basis of alignment data of MbtH-dependent CloH and MbtH-independent NovH (83% identity), a single mutation, L383 M, was made in CloH resulting in a mutant protein with some MbtH-independent ATP/PPi exchange activity.[20] However, the position corresponding to CloH L383 in all the nocardicin A-domains as well as all other MbtH protein dependent A-domains (Supporting Information, Figure S3) is a positively charged arginine residue (except for lysine in NocB A4), suggesting that the analogous mutation in A-domains other than CloH would not restore MbtH protein independent A-domain activity. Identification of a residue or set of residues that may account for the binding of NocI by A1, A2, and A4 but not A3 and A5 was not fruitful. A similar analysis, alignment of MbtH-independent L-Arg activating A6 domain from the lysobactin NRPS with the similar MbtH-dependent A2 domain from NocA (Supporting Information, Figure S4) also failed to suggest a MbtH protein binding site. The observation that NocP substituted for NocI for A_1T_1−His_6 and A_4T_4−His_6 but not for MBP−A_2T_2−His_6 suggests variability at the A-domain•MbtH interface, complicating prediction of interaction sites.

The discovery of the MbtH protein requirement for ATP/PPi exchange activity has been crucial for furthering the understanding of nocardicin A biosynthesis. As noted earlier, the structure of the nocardicins is characterized by the non-ribosomal tripeptide core D-*p*HPG−L-Ser−D-*p*HPG biosynthesized by NRPSs NocA and NocB comprising five modules, all essential for nocardicin A biosynthesis.[46] The heterologous expression and ATP/PPi exchange data for the modules of NocA and NocB validates the previous assumption that the tripeptide core derives from modules 3, 4, and 5.[24] The substrate specificities for MbtH-dependent A1 and A2, L-*p*HPG and L-Arg, respectively, have been of particular interest due to their absence in nocardicin A and in the case of A2 the inability to predict its substrate using bioinformatics or establish it experimentally.

Both in vivo and in vitro experimental evidence collected on NocA and NocB is consistent with a linear NRPS producing pentapeptide L-*p*HPG−L-Arg−D-*p*HPG−L-Ser−L-*p*HPG instead of a "Type C" NRPS model in which module skipping occurs to yield a tripeptide, as suggested previously.[24] The trimming of leader peptides from ribosomal protein products is well known in nature, but there are only a few examples of proteolysis in the biosynthesis of non-ribosomal natural products. The trimming of a leader peptide has been observed in xenocoumarin biosynthesis by periplasmic protease XcnG[47] and during didemnin biosynthesis by an unknown protease.[48] The excision of an N-terminal fatty acid chain added by an NRPS in pyoverdine biosynthesis by periplasmic protease PvdQ has been demonstrated[49] while a similar reaction is suspected in saframycin biosynthesis.[50] Although tabtoxin is not a non-ribosomal product, this β-lactam-containing prodrug is trimmed by periplasmic peptidase TapP to its active form.[51] The backbone of caerulomycin A is biosynthesized by a PKS−NRPS hybrid in which the terminal amino acid added in the final module, L-leucine, is removed later in the biosynthesis by a metallo-dependent amidohydrolase CrmL.[52]

The proteases discussed in the examples above, XcnG, PvdQ, TapP, and CrmL, are all encoded in their respective gene clusters. The only gene candidate resembling a protease in the nocardicin A gene cluster is NocK. NocK contains a catalytic triad consistent with a serine protease[53] and an N-terminal signal sequence predicting the export of this protein via the twin arginine translocation (Tat) pathway to the periplasm.[54,55] However, the definitive assignment of a proteolytic role for NocK is compromised by insertional inactivation experiments showing that *nocK* is not essential for nocardicin A biosynthesis in *N. uniformis.*[53] While the timing of the cleavage of the leader peptide is currently unclear as is any role the leader dipeptide might have in downstream reactions, biosynthetic logic dictates that, in nocardicin A biosynthesis, trimming of the N-terminal leader dipeptide occurs prior to oxime formation (catalyzed by NocL) at the N-terminus of the remaining tripeptide. Since the P450 catalyzed oxime reaction likely occurs in the cytoplasm, it seems unlikely that during nocardicin A biosynthesis, an intermediate would be exported to the periplasm for proteolysis

Scheme 1

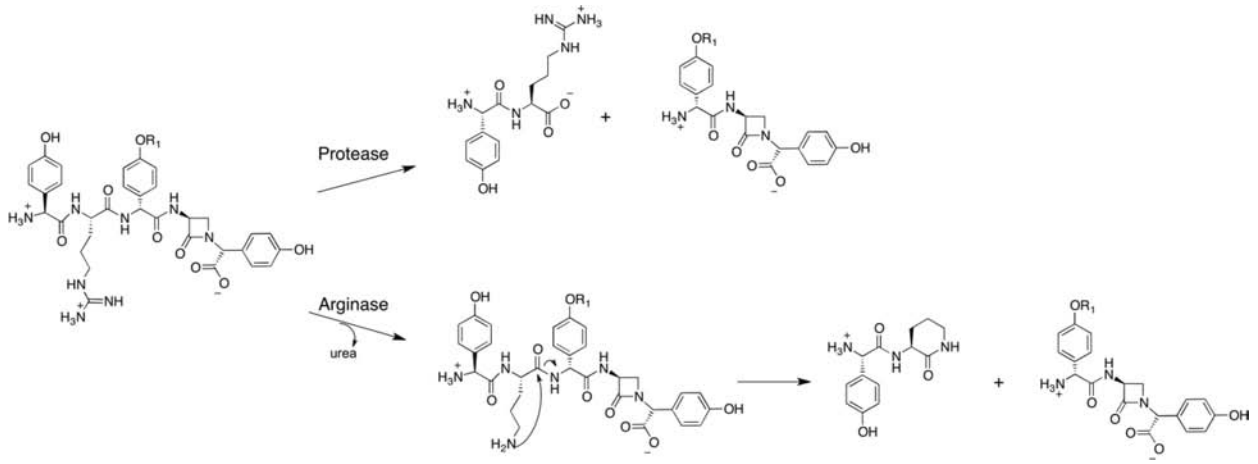

requiring the tripeptide intermediate to be imported back to the cytoplasm for reaction with NocL.

The identification of L-Arg as the preferred substrate for A2 leads to the possibility that the pentapeptide core is trimmed during nocardicin A biosynthesis by an ordinary cytoplasmic trypsin-like protease (Scheme 1). While trypsin, a serine protease, is more commonly known as mammalian digestive enzyme, it has also been identified in a wide range of organisms including *Streptomyces*.[29] Analysis of the nocardicin A gene cluster, 15 kbp of the upstream nucleotide sequence and ~5 kbp of the downstream nucleotide sequence, failed to elucidate a gene encoding a trypsin protease. Phylogenic classification of the *N. uniformis* strain used in these studies based on 16S rDNA was performed to determine if *N. uniformis* was similar to the nocardicin A producing *A. mirum* strain that has been fully sequenced. Unexpectedly, the 16S rDNA of these two strains were found to be identical, supporting the previous observation that *N. uniformis* strain ATCC 21806 formed synnemata and zoospores highly similar to *A. mirum*.

A BLAST-P search of the *A. mirum* genome for proteins similar to the well-characterized *S. griseus* and *S. erythraeus* trypsins identified three proteins with greater than 38% identity and greater than 50% similarity and several others of lower identity and similarity.[30,32] The conserved catalytic triad and substrate specificity pocket characteristic of trypsin is observed in the protein sequence alignment of the putative *A. mirum* trypsin proteases.[29] (Supporting Information, Figure S5) These proteins are not encoded in the defined nocardicin A gene cluster but may be available to the nocardicin A biosynthetic pathway due to their constitutive expression or cross-talk between gene clusters as observed in the erythrochelin and rhodochelin biosynthetic pathways.[56−58] Cross-talk between gene clusters has been proposed to occur in *A. mirum* during the biosynthesis of the siderophore mirubactin.[59] The presence of trypsin and the ability of bovine trypsin to cleave the predicted pentapeptide product, L-*p*HPG−L-Arg−D-*p*HPG−L-Ser−L-*p*HPG, at the C-terminal site of the L-Arg residue supports this hypothesis.

Although whole cell incorporation experiments with a linear peptide would likely result in proteolysis of the peptide by nutrient uptake systems, two experiments were performed in which either peptide L-*p*HPG−L-Arg−D-*p*HPG−L-Ser−L-*p*HPG or its D-isomer peptide L-*p*HPG−L-Arg−D-*p*HPG−L-Ser−D-*p*HPG was added to the fermentation culture of a previously characterized *N. uniformis* point mutant, *nocB* S571A, in which the NRPS is inactivated. Unfortunately, nocardicin A production was not observed with either peptide, but peaks correlated to 4-mer and 3-mer degradation products were observed, consistent with proteolytic degradation from the N-terminus.

An alternative, self-cleavage mechanism is also proposed in Scheme 1. Conversion of the second position L-Arg to L-Orn by an arginase could lead to cyclization by attack of the side chain amine of L-Orn on the amide carbonyl. This would result in self-cleavage at the C-terminus of L-Arg, liberating the tripeptide core of the nocardicins as previously suggested.[24]

■ CONCLUSION

In conclusion, MbtH protein dependence of A-domain activity was observed in A1, A2, and A4 of the nocardicin A NRPSs, while A3 and A5 showed no such requirement. The two MbtH proteins associated with or near the cluster were found to be not completely complementary, indicating that interaction with an A-domain is more complex than simple association with the three conserved tryptophan residues characteristic of MbtH proteins. Analysis of coexpressed protein complexes indicates a 1:1 stoichiometry between A-domains A1 and A4 with NocI. This discovery enabled the determination of the substrate amino acid specificity for each A-domain using the ATP/PPi exchange assay to yield a predicted product, L-*p*HPG−L-Arg−D-*p*HPG−L-Ser−L-*p*HPG, for the nocardicin NRPS. The requirement for truncation of this pentapeptide and the absence of a protease in the nocardicin A gene cluster that could perform such a function led to the proposal of a self-cleavage mechanism or the action of a protease encoded outside the gene cluster. Classical morphological criteria that have suggested *N. uniformis* ATCC 21806 should be reclassified as *A. mirum* were confirmed by direct comparison of their 16S rDNA sequences and the mutual identity of three candidate trypsin-encoding genes. Cross-talk with these enzymes or other endo- or exoproteases can be invoked to account for truncation to the tripeptide core of the nocardicins. With the identity of a putative pentapeptide precursor in hand and the availability of a sequenced genome, the way is open to address the central timing and mechanistic questions of peptide processing, β-lactam formation, and C-terminal epimerization.

dx.doi.org/10.1021/ja307710d | *J. Am. Chem. Soc.* 2013, 135, 1749−1759

Table 1. Oligonucleotide Primers Used for NRPS Expression Vector Construction

description	label	primer sequence (5′ to 3′)
A_1T_1	M1 For (*Nco*I)	GCGCCATGGGGGACAGCGAGGAGTGGGAGCGC
	M1 Rev (*Xho*I)	GCGCTCGAGGGCCAGCTCCTCGATCCGCCTGGCCAG
A_2T_2	M2 For (*Nco*I)	GCCCATGGTTAGCACCGGCGCGCCGGTCGAACC
	M2 Rev (*Bam*HI)	GCGGATCCCGCGTCGTCGGCCCACGGC
A_3T_3 E_3C_4	M3 For (*Nco*I)	TCTTCCATGGTGCTCGGGGACGAC
	M3 Rev (*Bam*HI)	TATAGGATCCCGGGTTCCTTCTCCCCTCG
A_4T_4	M4 For (*Nco*I)	GCCCCATGGCCTTTCGAGTGCGCGACCTGTTCGCCG
	M4 Rev (*Xho*I)	GGCCTCGAGGGTGGACGCCTCGTCGGCG
$C_5A_5T_5TE$	M5 For (*Nco*I)	GCGCTCCATGGACGAGGAGGCGCTGCTGGCG
	M5 Rev	TATAAAGCTTCCGCTCTCCTCCCAGCGCGC

Table 2. Oligonucleotide Primers Used for NocI and NocP Expression Vector Construction

vector	label	primer sequence (5′ to 3′)
pCDFDuet	NocI For (*Nco*I)	GCCCCATGGTGGGAGAGAACGAGGATTCCGG
	NocI Rev (*Hin*dIII)	GCGAAGCTTTCAAGCCCGGTCCCCGGCC
pTYB12	NocI For (*Bsm*I)	GCCGAATGCTCTGGGAGAGAACGAGGATTCCGG
	NocI Rev (*Xho*I)	GCGCTCGAGTCAAGCCCGGTCCCCGGCC
pET28b(+)	NocP For (*Nde*I)	GCGGCATATGAACCCCTTCGACGACCACGACCGCGCT
	NocP Rev (*Xho*I)	GCGCTCGAGTCAGGCGTCGGGGTCGGGCGCGCCCGCGCG
pCDFDuet	NocP For (*Nde*I)	GCGGCATATGAACCCCTTCGACGACCACGACCGCGCT
	NocP Rev (*Xho*I)	GCGCTCGAGTCAGGCGTCGGGGTCGGGCGCGCCCGCGCG

EXPERIMENTAL METHODS

Cloning of NRPS Expression Vectors. The primers used for the PCR amplification of the coding region of each multidomain construct are described in Table 1. Amplification from previously prepared plasmids was performed using Pfu (Agilent Technologies, Santa Clara, CA), Pfu Turbo (Agilent), or KOD (EMD Biosciences, Gibbstown, NJ) DNA polymerases. For modules 1 and 4, the PCR products were digested with *Nco*I and *Xho*I and directly ligated into the *Nco*I/*Xho*I site in pET28b(+) (EMD Biosciences). For module 2, the PCR product was digested with *Nco*I and *Bam*HI and directly ligated into the *Nco*I/*Bam*HI site in pET28b(+). For cloning into pMALc2x (New England Biolabs, Ipswich, MA), the *Nco*I/*Blp*I fragment was excised from pET28b(+) blunted with a Klenow reaction and ligated into the Klenow blunted *Eco*RI/*Hin*dIII site of pMALc2x. The PCR product for module 3 was digested and directly ligated into the *Nco*I/*Bam*HI site of pQE60 (Qiagen, Valencia, CA). The module 3-histidine tag coding sequence was digested from pQE60 with *Nco*I/*Hin*dIII for ligation into the *Nco*I/*Hin*dIII site of pET28b(+). The PCR product encoding module 5 was subcloned into pCRBlunt (Life Technologies, Grand Island, NY). The coding region was excised from pCRBlunt with a *Nco*I/*Hin*dIII digest and ligated into the *Nco*I/*Hin*dIII site of pET28b(+). All constructs were confirmed by sequencing analysis performed by the Biosynthesis and Sequencing Facility, Johns Hopkins Medical School, Baltimore, MD.

Cloning of NocI and NocP Expression Vectors. The *nocI* gene was amplified by PCR from cosmid DNA using KOD DNA polymerase and the primers listed in Table 2. PCR products were subcloned into pCRBlunt or pJET1.2 (ThermoFisher Scientific, Waltham, MA), confirmed by sequencing prior to excision, and ligation into pCDFDuet (EMD Biosciences) and pTYB12 (New England Biolabs), respectively, using the cut sites indicated. The *nocP* gene was similarly amplified by PCR from cosmid DNA using KOD DNA polymerase and the primers listed in Table 2. PCR products were directly cloned into the *Nde*I/*Xho*I sites of pET28b(+) and pCDFDuet, respectively.

Heterologous Expression and Purification of NRPS Modules. Seed cultures consisting of 50 mL of LB medium with 25 μg/mL kanamycin for pET28 constructs or 100 μg/mL for pMALc2x constructs and 34 μg/mL chloramphenicol inoculated with *E.coli* BL21(DE3) Rosetta2 (EMD Biosciences) transformed with expression vector were grown overnight at 37 °C with shaking. The growth medium, 2xYT (3 L) supplemented with 5 mM $MgCl_2$, 25 μg/mL kanamycin or 100 μg/mL ampicillin, and 34 μg/mL chloramphenicol, was inoculated with the seed culture at a ratio of 1:100. Cells were grown at 37 °C with shaking until the OD_{600} measured ∼0.6. Growth cultures were cooled to 17.5 °C prior to induction of protein expression with the addition of isopropyl β-D-1-thiogalactopyranoside (IPTG; 1 mM final concentration for pET28b, 0.3 mM for pMALc2x). Expression was continued overnight at 17.5 °C. Cells were collected by centrifugation (5180*g*, 10 min at 4 °C), resuspended in lysis buffer (50 mM NaH_2PO_4 pH = 8, 300 mM NaCl, 10 mM imidazole, 10% glycerol), and lysed by sonication. The cell debris was collected by centrifugation at 37044*g* and 4 °C for 30 min. NTA resin (Qiagen) was added to the lysate and allowed to incubate at 4 °C with turning for at least 1 h. The lysate−resin slurry was poured into an empty column. The resin was washed with lysis buffer followed by wash buffer (50 mM NaH_2PO_4 pH = 8, 300 mM NaCl, 20 mM imidazole, 10% glycerol). The His_6-tagged protein was eluted with 4−10 mL of elution buffer (50 mM NaH_2PO_4 pH = 8, 300 mM NaCl, 250 mM imidazole, 10% glycerol).

Protein isolated by affinity chromatography was dialyzed in 3 × 1 L dialysis buffer (50 mM Tris−HCl pH = 7.5 at 4 °C, 50 mM NaCl, 5 mM $MgCl_2$, 1 mM DTT, 10% glycerol), with 1 h for each exchange. For further purification of modules 1, 3, 4, and 5, the protein solution was loaded onto a 5 mL HiTrapQ cartridge (GE Life Sciences, Pittsburgh, PA) pre-equilibrated with dialysis buffer (50 mM NaCl) using an ÄKTA FPLC (GE Life Sciences). Fractions were collected as the 50−500 mM NaCl (300 mL total volume) gradient was applied to elute adsorbed proteins at a flow rate of ∼1 mL/min with UV detection at 280 nm. Fractions (3 mL) were collected and analyzed by SDS-PAGE. Fractions containing the target fusion protein were collected, concentrated to greater than 2 mg protein/mL using a centrifugal filter (Millipore Corp., Billerica, MA), and flash frozen in liquid nitrogen for storage at −80 °C.

Heterologous Expression and Isolation of Untagged NocI. Seed cultures consisting of 50 mL of LB medium with 100 μg/mL ampicillin were inoculated with *E.coli* BL21(DE3) transformed with the pTYB12/*nocI* expression vector and grown overnight at 37 °C with shaking. Six flasks, each containing 0.5 L of LB medium with 100 μg/mL ampicillin and inoculated with 5 mL of seed culture, were grown at 37 °C and 180 rpm until an OD_{600} value of ∼0.6 and then cooled to 10 °C (1 h). IPTG, final concentration 0.5 mM, was added

to induce protein expression. Expression was continued at 17.5 °C overnight with shaking.

The following steps were performed at ≤4 °C. The next day, cells were pelleted by centrifugation (5180*g*, 10 min) and then resuspended in 150 mL of lysis buffer (20 mM Tris−HCl pH = 8, 500 mM NaCl, 1 mM EDTA). Cells were lysed by sonication, and the cell debris was removed by centrifugation. Chitin resin (New England Biolabs no. E6900S), 10 mL, was conditioned with ∼110 mL of column buffer (50 mM Tris−HCl pH = 8, 50 mM NaCl, 10% glycerol). The clarified cell lysate was passed through the chitin bead column at a flow rate of ∼1 mL/min. The column was then washed with 100 mL of column buffer. When the level of the wash buffer was close to the top of the resin, 20 mL of cleavage buffer (100 mM DTT in column buffer) was added to the column. The column was capped, and the resin was resuspended in the cleavage buffer and incubated at 4 °C for 72 h. The column eluate was collected. An additional 10 mL of cleavage buffer was applied to the column, eluted, and combined with the previous eluate. The 30 mL of column eluate was filtered using an Amicon (Millipore Corp.) Ultra 30 kDa MWCO centrifuge filter. The flow-through was collected and concentrated using an Amicon Ultra 3 kDa MWCO filter. Native NocI (untagged) was flash frozen in liquid nitrogen for storage in the −80 °C freezer.

Coexpression of Module (His_6-Tagged) and NocI or NocP (Untagged). Each module expression plasmid (pET28/Mx or pMALc2x/M2) was cotransformed with pCDFDuet/*nocI* (untagged) into *E.coli* BL21(DE3) Rosetta 2 using standard electroporation protocols. Conditions for growth, expression, and isolation by NTA affinity chromatography were similar to those given for the heterologous expression of individual modules above, except that 50 μg/mL spectinomycin was added to the seed culture and growth culture medium to maintain selection for the pCDFDuet/*nocI* expression vector. In addition, NTA chromatography was the terminal step in the isolation, that is, further purification by ion-exchange chromatography was not done.

ATP/PPi Exchange Assay. Each 100 μL reaction consisted of 36.3 mM HEPES pH = 7.5, 0.15 mM EDTA, 7.25 mM $MgCl_2$, 1.5 mM DTT, 3.7 mM ATP, 7.3% (v/v) glycerol, 0.75 mM amino acid substrate, and 1 mM $Na_4P_2O_7$ with 1 μCi ^{32}P-labeled $Na_4P_2O_7$ (NEN Perkin−Elmer, Waltham, MA). The reaction was initiated by the addition of the protein (0.5−5 μM). Following incubation at room temperature for 30 min, the reaction was quenched by the addition of 400 μL of 0.5 M $HClO_4$ and chased with 400 μL of 100 mM sodium pyrophosphate (unlabeled); then, 200 μL of a 4% (w/v) suspension of activated charcoal (Norit A) was added. The charcoal was pelleted by centrifugation (14 000 rpm, 5 min), washed twice with 1 mL of water, and repelleted by centrifugation. The charcoal pellet was resuspended in 500 mL of water, transferred to a 7 mL glass scintillation vial, and mixed with 5 mL of Optifluor (NEN Perkin−Elmer). Each sample was measured using a Beckman model LS6500 scintillation counter (Beckman Coulter, Brea, CA).

Modified ATP/PPi Exchange Assay for Module 2. Each 200 μL reaction mixture consisted of 50 mM Tris−HCl pH = 7.5, 10 mM $MgCl_2$, 5 mM amino acid substrate, 2.5 mM $Na_4P_2O_7$ with 2 μCi ^{32}P-labeled $Na_4P_2O_7$, and 5 μM protein. Prior to the addition of ATP, the reaction mixture was incubated at 30 °C for 10 min. Following this preincubation, 2.5 mM ATP was added to initiate the ATP/PPi exchange reaction, and the mixture was incubated at 30 °C for an additional 30 min. The exchange reaction was quenched with acid and prepared for scintillation counting using the procedure outlined in the previous section.

Determination of Module/NocI Stoichiometry by HPLC. Samples isolated by NTA affinity chromatography were denatured by the addition of 8 M urea (Sigma−Aldrich, St. Louis, MO) to a final concentration of 6 M urea and incubated at room temperature for 30 min. Following incubation, samples were diluted with water for a final concentration of 2 M urea. Samples were analyzed by protein HPLC, employing an Agilent 1200 HPLC system equipped with a diode array detector. Filtered denatured protein solutions (100 μL) in 2 M urea were injected onto a Vydac C4 protein column (150 mm × 46 mm) (W.R. Grace & Co., Columbia, MD) heated to 70 °C. The flow rate was 1 mL/min. Proteins were eluted using a binary gradient in which mobile phase A consisted of 90:10 water/acetonitrile (ACN) with 0.1% trifluoroacetic acid (TFA) and mobile phase B consisted of 90:10 ACN/water with 0.1% TFA. After 3 min at 82:18 A/B, a linear gradient to 50:50 A/B over 45 min was programmed. Proteins were detected by monitoring absorbance at 280 nm and were quantified by integration using OriginPro v.8.6 software (OriginLab, Northampton, MA). The molar absorptivity for each protein was calculated using Vector NTI software (Life Technologies).

Conditions for Proteolysis and HPLC Analysis. Peptide L-*p*HPG−L-Arg−D-*p*HPG−L-Ser−L-*p*HPG was procured from Peptide 2.0, Inc. (Chantilly, VA) for testing. In a total reaction volume of 100 μL, 200 nmol of pentapeptide was reacted with 20 μg of modified (TPCK-treated) trypsin (New England Biolabs) in buffer containing 50 mM Tris−HCl, pH = 8 at 25 °C, and 20 mM $CaCl_2$. The reaction was incubated at 37 °C overnight. Trypsin was removed from the reaction by filtration through a 3 kDa MWCO centrifugal filter (Millipore), and the flow-through was analyzed by an Agilent 1100 HPLC equipped with a diode array detector. Aliquots of the reaction mixture were injected onto a Luna C18(2) column (250 mm × 46 mm) (Phenomenex, Torrence, CA) using a binary gradient in which mobile phase A consisted of 0.1% TFA in water and mobile phase B consisted of 90:10 ACN/water with 0.1% TFA. After 5 min at 94:6 A/B and a flow rate of 1 mL/min, a linear gradient to 85:15 A/B over 15 min was programmed.

LC-MS analysis was conducted using an Agilent 1200 series, 6220 LC-MS/TOF analyzer equipped with a dual electrospray ionization (ESI) source operated in positive mode under the following conditions: fragmentor, 135 V; skimmer, 65 V; gas temperature, 350 °C; drying gas, 12 L/min; nebulizer, 40 psi; and Vcap, 3500 V for mass range 100−1700 *m*/*z*. Separations were performed with a Zorbax C18 5 μm column (150 mm × 4.6 mm) at 30 °C using a binary gradient in which mobile phase A consisted of 0.1% formic acid in water and mobile phase B consisted of 90:10 ACN/water with 0.1% formic acid. A linear gradient elution from 6% to 85% mobile phase B over 15 min was programmed. An aliquot of the trypsin reaction mixture described above was diluted 1:100 with 0.1% formic acid in water and 5 μL was injected for LC-MS analysis.

Pentapeptide Feeding Experiment. The preparation and growth conditions for the *N. uniformis nocB* S571A mutant has been described previously.[46] *N. uniformis* is maintained on ISP2 solid medium (Difco Laboratories, Detroit, MI) at 28 °C. Seed cultures were prepared in TSB medium (Difco Laboratories) and grown to saturation at 28 °C with shaking. Nocardicin fermentation medium[60] was inoculated with 2 mL of the starter seed culture and incubated at 28 °C with shaking. Following 34 h of incubation, the culture medium was supplemented with peptide L-*p*HPG−L-Arg−D-*p*HPG−L-Ser−L-*p*HPG or peptide L-*p*HPG−L-Arg−D-*p*HPG−L-Ser−D-*p*HPG (Peptide 2.0, Inc., Chantilly, VA) to a final concentration of 5 mM. The supplemented mutant *N. uniformis* cultures were incubated for an additional day. Upon completion, the cultures were centrifuged to separate the cell mass from the supernatant, analyzed by HPLC, and stored at −20 °C. HPLC analysis to detect nocardicin A was performed as described previously.[46] A second HPLC analysis for the detection of novel metabolites was performed using the same HPLC system and a Luna C18(2) column (Phenomenex, Torrance, CA). For this analysis, the binary mobile phase solutions were as follows: A, 0.1% TFA in water; B, 90:10 ACN/water with 0.1% TFA. Filtered culture supernatants (10 μL) were directly injected and eluted with a shallow gradient starting with a ratio of 94:6 (A/B) for 5 min to a ratio of 85:15 (A/B) at 20 min and ending with a ratio of 60:40 (A/B) at 40 min. Analytes were detected at 272 nm with a diode array detector.

Phylogenic Analysis of *N. uniformis* ATCC 21806. The isolation of genomic DNA from *N. uniformis* subsp. *tsuyamanensis* ATCC 21806 was carried out according to the standard techniques from Practical Streptomyces Genetics.[61] Amplification of 16S rDNA was performed using the universal 16S rDNA primers fD1 and rp2[62] with KOD DNA polymerase. PCR products were subcloned into pJET1.2 and submitted for sequencing at the Biosynthesis and Sequencing Facility, Johns Hopkins Medical School, Baltimore, MD.

The resulting sequences were compared with those available in the GenBank database maintained by the National Center for Biotechnology Information (NCBI) using the BLASTN algorithm.[30]

PCR Amplification of Trypsin Coding Sequences from *N. uniformis*. Using the Primer-BLAST[63] algorithm on the NCBI web site, primers (Table 3) were designed to amplify regions encoding three trypsins proteases predicted to be present in *N. uniformis* based on the *A. mirum* genome. Targeted genes were amplified from gDNA isolated *N. uniformis* using KOD DNA polymerase. PCR products were subcloned into pJET1.2 and submitted for sequencing analysis.

Table 3

trypsin primer set	primer sequence (5′ to 3′)
ACU39320 - forward	GGACATTGCGGTGGTGGAAGACGTTC
ACU39320 - reverse	GGAAGGAGATGAGCATGGCGGAAACC
ACU39665 - forward	CGCGCTCAGCACGCTGTAGTAGG
ACU39665 - reverse	GAAAGGAACTCCGATGGCGAAAACCCT
ACU39678 - forward	CATCAGAGTCCGCATACCGGCCAAC
ACU39678 - reverse	ATCGACCTGGTCTTTCAGGGCTAACCT

■ ASSOCIATED CONTENT

Ⓢ Supporting Information

HPLC chromatograms and mass analysis for the trypsinolysis reaction of pentapeptide L-*p*HPG–L-Arg–D-*p*HPG–L-Ser–L-*p*HPG and protein sequence alignments. This material is available free of charge via the Internet at http://pubs.acs.org.

■ AUTHOR INFORMATION

Corresponding Author

ctownsend@jhu.edu

Present Address

[†]Department of Chemistry, Adrian College, Adrian, Michigan 49221, United States.

Notes

The authors declare no competing financial interest.

■ ACKNOWLEDGMENTS

This work was supported by NIH grant AI014937. The Greenberg group (JHU) is thanked for use of their FPLC and support for radiochemical experiments. Dr. W. E. Bocik performed the initial subcloning of *nocI*, and we thank Prof. D. I. Barrick (Biophysics, JHU) for helpful discussions. Prof. P. F. Leadlay (Cambridge) kindly provided samples of L-*δ*-*N*-hydroxyornithine and L-*δ*-*N*-acetyl-*δ*-*N*-hydroxyornithine for the ATP/PPi exchange assays. Drs. A. C. Jacobs and I. P. Mortimer are acknowledged for their help with MALDI and ESI-MS measurements. Mr. E. Philander (Analytical Sciences Group, McCormick & Co., Inc.) kindly performed the LC-MS analyses described in this manuscript.

■ REFERENCES

(1) Felnagle, E. A.; Jackson, E. E.; Chan, Y. A.; Podevels, A. M.; Berti, A. D.; McMahon, M. D.; Thomas, M. G. *Mol. Pharmaceutics* **2008**, *5*, 191–211.

(2) Lai, J. R.; Fischbach, M. A.; Liu, D. R.; Walsh, C. T. *J. Am. Chem. Soc.* **2006**, *128*, 11002–11003.

(3) Walsh, C.; Chen, H.; Keating, T.; Hubbard, B.; Losey, H.; Luo, L.; Marshall, C.; Miller, D.; Patel, H. *Curr. Opin. Chem. Biol.* **2001**, *5*, 525–534.

(4) Sattely, E. S.; Fischbach, M. A.; Walsh, C. T. *Nat. Prod. Rep.* **2008**, *25*, 757–793.

(5) Hahn, M.; Stachelhaus, T. *Proc. Natl. Acad. Sci. U.S.A.* **2004**, *101*, 15585–15590.

(6) Quadri, L. E. N.; Sello, J.; Keating, T. A.; Weinreb, P. H.; Walsh, C. T. *Chem. Biol.* **1998**, *5*, 631–645.

(7) Lautru, S.; Oves-Costales, D.; Pernodet, J.-L.; Challis, G. L. *Microbiology* **2007**, *153*, 1405–1412.

(8) Wolpert, M.; Gust, B.; Kammerer, B.; Heide, L. *Microbiology* **2007**, *153*, 1413–1423.

(9) Drake, E. J.; Cao, J.; Qu, J.; Shah, M. B.; Straubinger, R. M.; Gulick, A. M. *J. Biol. Chem.* **2007**, *282*, 20425–20434.

(10) Buchko, G. W.; Kim, C.-Y.; Terwilliger, T. C.; Myler, P. J. *Tuberculosis* **2010**, *90*, 245–251.

(11) Heemstra, J. R.; Walsh, C. T.; Sattely, E. S. *J. Am. Chem. Soc.* **2009**, *131*, 15317–15329.

(12) Conti, E.; Stachelhaus, T.; Marahiel, M. A.; Brick, P. *EMBO J.* **1997**, *16*, 4174–4183.

(13) Challis, G. L.; Ravel, J.; Townsend, C. A. *Chem. Biol.* **2000**, *7*, 211–224.

(14) Stachelhaus, T.; Mootz, H. D.; Marahiel, M. A. *Chem. Biol.* **1999**, *6*, 493–505.

(15) Rausch, C.; Weber, T.; Kohlbacher, O.; Wohlleben, W.; Huson, D. H. *Nucleic Acids Res.* **2005**, *33*, 5799–5808.

(16) Röttig, M.; Medema, M. H.; Blin, K.; Weber, T.; Rausch, C.; Kohlbacher, O. *Nucleic Acids Res.* **2011**, *39*, W362–W367.

(17) Prieto, C.; García-Estrada, C.; Lorenzana, D.; Martín, J. F. *Bioinformatics* **2012**, *28*, 426–427.

(18) Felnagle, E. A.; Barkei, J. J.; Park, H.; Podevels, A. M.; McMahon, M. D.; Drott, D. W.; Thomas, M. G. *Biochemistry* **2010**, *49*, 8815–8817.

(19) Zhang, W.; Heemstra, J. R.; Walsh, C. T.; Imker, H. J. *Biochemistry* **2010**, *49*, 9946–9947.

(20) Boll, B.; Taubitz, T.; Heide, L. *J. Biol. Chem.* **2011**, *286*, 36281–36290.

(21) Watanabe, K.; Okuda, T.; Yokose, K.; Furumai, T.; Maruyama, H. B. *J. Antibiot.* **1983**, *36*, 321–324.

(22) Hasegawa, T.; Lechevalier, M. P.; Lechevalier, H. A. *Int. J. Syst. Bacteriol.* **1978**, *28*, 304–310.

(23) Townsend, C. A.; Brown, A. M. *J. Am. Chem. Soc.* **1983**, *105*, 913–918.

(24) Gunsior, M.; Breazeale, S. D.; Lind, A. J.; Ravel, J.; Janc, J. W.; Townsend, C. A. *Chem. Biol.* **2004**, *11*, 927–938.

(25) Rausch, C.; Hoof, I.; Weber, T.; Wohlleben, W.; Huson, D. H. *BMC Evol. Biol.* **2007**, *7*, 78.

(26) Hou, J.; Robbel, L.; Marahiel, M. A. *Chem. Biol.* **2011**, *18*, 655–664.

(27) Schlaberg, R.; Simmon, K. E.; Fisher, M. A. *Emerging Infect. Dis.* **2012**, *18*, 422–430.

(28) Drancourt, M.; Bollet, C.; Carlioz, A.; Martelin, R.; Gayral, J.-P.; Raoult, D. *J. Clin. Microbiol.* **2000**, *38*, 3623–3630.

(29) Rypniewski, W. R.; Perrakis, A.; Vorgias, C. E.; Wilson, K. S. *Protein Eng.* **1994**, *7*, 57–64.

(30) Altschul, S.; Madden, T.; Schaffer, A.; Zhang, J.; Zhang, Z.; Miller, W.; Lipman, D. *Nucleic Acids Res.* **1997**, *25*, 3389–3402.

(31) Stosová, T. á.; Sebela, M.; Rehulka, P.; Sedo, O.; Havlis, J.; Zdráhal, Z. *Anal. Biochem.* **2008**, *376*, 94–102.

(32) Kiser, J. Z.; Post, M.; Wang, B.; Miyagi, M. *J. Proteome Res.* **2009**, *8*, 1810–1817.

(33) Drake, E. J.; Nicolai, D. A.; Gulick, A. M. *Chem. Biol.* **2006**, *13*, 409–419.

(34) Yonus, H.; Neumann, P.; Zimmermann, S.; May, J. J.; Marahiel, M. A.; Stubbs, M. T. *J. Biol. Chem.* **2008**, *283*, 32484–32491.

(35) Du, L.; He, Y.; Luo, Y. *Biochemistry* **2008**, *47*, 11473–11480.

(36) Osman, K. T.; Du, L.; He, Y.; Luo, Y. *J. Mol. Biol.* **2009**, *388*, 345–355.

(37) Mitchell, C. A.; Shi, C.; Aldrich, C. C.; Gulick, A. M. *Biochemistry* **2012**, *51*, 3252–3263.

(38) Reger, A. S.; Wu, R.; Dunaway-Mariano, D.; Gulick, A. M. *Biochemistry* **2008**, *47*, 8016–8025.

(39) Branchini, B. R.; Rosenberg, J. C.; Fontaine, D. M.; Southworth, T. L.; Behney, C. E.; Uzasci, L. *J. Am. Chem. Soc.* **2011**, *133*, 11088−11091.
(40) Sundlov, J. A.; Fontaine, D. M.; Southworth, T. L.; Branchini, B. R.; Gulick, A. M. *Biochemistry* **2012**, *51*, 6493−6495.
(41) Borisova, S. A.; Liu, H.-w. *Biochemistry* **2010**, *49*, 8071−8084.
(42) Moncrieffe, M. C.; Fernandez, M.-J.; Spiteller, D.; Matsumura, H.; Gay, N. J.; Luisi, B. F.; Leadlay, P. F. *J. Mol. Biol.* **2012**, *415*, 92−101.
(43) Imker, H. J.; Krahn, D.; Clerc, J.; Kaiser, M.; Walsh, C. T. *Chem. Biol.* **2010**, *17*, 1077−1083.
(44) Zolova, O. E.; Garneau-Tsodikova, S. *MedChemComm* **2012**, *3*, 950−955.
(45) McMahon, M. D.; Rush, J. S.; Thomas, M. G. *J. Bacteriol.* **2012**, *194*, 2809−2818.
(46) Davidsen, J. M.; Townsend, C. A. *Chem. Biol.* **2012**, *19*, 297−306.
(47) Reimer, D.; Pos, K. M.; Thines, M.; Grun, P.; Bode, H. B. *Nat. Chem. Biol.* **2011**, *7*, 888−890.
(48) Xu, Y.; Kersten, R. D.; Nam, S. J.; Lu, L.; Al-Suwailem, A. M.; Zheng, H. J.; Fenical, W.; Dorrestein, P. C.; Moore, B. S.; Qian, P. Y. *J. Am. Chem. Soc.* **2012**, *134*, 8625−8632.
(49) Drake, E. J.; Gulick, A. M. *ACS Chem. Biol.* **2011**, *6*, 1277−1286.
(50) Koketsu, K.; Watanabe, K.; Suda, H.; Oguri, H.; Oikawa, H. *Nat. Chem. Biol.* **2010**, *6*, 408−410.
(51) Levi, C.; Durbin, R. D. *Physiol. Mol. Plant Pathol.* **1986**, *28*, 345−352.
(52) Zhu, Y. G.; Fu, P.; Lin, Q. H.; Zhang, G. T.; Zhang, H. B.; Li, S. M.; Ju, J. H.; Zhu, W. M.; Zhang, C. S. *Org. Lett.* **2012**, *14*, 2666−2669.
(53) Kelly, W. L.; Townsend, C. A. *J. Bacteriol.* **2005**, *187*, 739−46.
(54) Petersen, T. N.; Brunak, S.; von Heijne, G.; Nielsen, H. *Nat. Methods* **2011**, *8*, 785−786.
(55) Bendtsen, J.; Nielsen, H.; Widdick, D.; Palmer, T.; Brunak, S. *BMC Bioinf.* **2005**, *6*, 167.
(56) Lazos, O.; Tosin, M.; Slusarczyk, A. L.; Boakes, S.; Cortés, J.; Sidebottom, P. J.; Leadlay, P. F. *Chem. Biol.* **2010**, *17*, 160−173.
(57) Robbel, L.; Helmetag, V.; Knappe, T. A.; Marahiel, M. A. *Biochemistry* **2011**, *50*, 6073−6080.
(58) Bosello, M.; Robbel, L.; Linne, U.; Xie, X.; Marahiel, M. A. *J. Am. Chem. Soc.* **2011**, *133*, 4587−4595.
(59) Giessen, T. W.; Franke, K. B.; Knappe, T. A.; Kraas, F. I.; Bosello, M.; Xie, X.; Linne, U.; Marahiel, M. A. *J. Nat. Prod.* **2012**, *75*, 905−914.
(60) Reeve, A. M.; Breazeale, S. D.; Townsend, C. A. *J. Biol. Chem.* **1998**, *273*, 30695−30703.
(61) Kieser, T.; Bibb, M. J.; Buttner, M. J.; Chater, K. F.; Hopwood, D. A. *Practical Streptomyces Genetics*; The John Innes Foundation: Norwich, U.K., 2000.
(62) Weisburg, W. G.; Barns, S. M.; Pelletier, D. A.; Lane, D. J. *J. Bacteriol.* **1991**, *173*, 697−703.
(63) Ye, J.; Coulouris, G.; Zaretskaya, I.; Cutcutache, I.; Rozen, S.; Madden, T. *BMC Bioinf.* **2012**, *13*, 134−145.